Numerical Methods for the solution of Hyperbolic Conservation Laws

A. Mazzia *

Abstract. In this paper we consider numerical approximations of hyperbolic conservation laws in the one-dimensional scalar case, by studying Godunov and van Leer's methods. Before to present the numerical treatment of hyperbolic conservation laws, a theoretical introduction is given together with the definition of the Riemann problem. Next the numerical schemes are discussed. We also present numerical experiments for the linear advection equation and Burgers' equation. The first equation is used for modeling discontinuities in fluid dynamics; the second one is used for modeling shocks and rarefaction waves. In this way we can compare the different behavior of both schemes.

Key words. Hyperbolic Conservation Laws, Riemann problem, Godunov's method, van Leer's method, limiter, Burgers' equation

1 Introduction

The mathematical description of many practical problems in science and engineering leads to conservation laws, that is time-dependent systems of partial differential equations (PDEs), usually hyperbolic and nonlinear, with a particularly simple structure. Fluid and gas dynamics, relativity theory, quantum mechanics, aerodynamics, meteorology, astrophysics - this is just a partial list of subjects where conservation laws apply. The study of numerical solution of hyperbolic conservations laws is an important and interesting field of research because there are special difficulties associated with solving these PDEs (i.e. shock formation, discontinuous solutions) and numerical methods based on simple finite-difference approximations may behave well for smooth solutions but can give disastrous results when discontinuities and shocks are present(see [5]). So, the study of linear conservation laws is important for understanding the behavior of a numerical scheme, but it is also very important to consider that the introduction of the nonlinearity changes dramatically the nature of the problem because it induces a loss of the uniqueness of the weak solution ([8, 9]). The weak solution that is physically relevant has then to be properly characterized and the numerical approximations have to respect this characterization otherwise they would converge to a weak solution which has no physical meaning. Therefore, the study of numerical approximations for nonlinear conservation laws is quite difficult. However, in the case of scalar conservation laws many important issues are well understood. In fact, since the numerical difficulties encountered with systems of equations in one or multidimensional space are already encountered in the one-dimensional scalar case, historically numerical schemes were first derived for scalar conservation laws. Only when they proved to perform well in this setting, they were extended to systems of conservation laws.

*Dipartimento di Metodi e Modelli Matematici per le Scienze Applicate, Via Belzoni 7, 35131 Padova, Italy. E-mail: amazzia@math.unipd.it

Therefore, we will treat only hyperbolic scalar conservation laws: the equations take the form

$$\frac{\partial}{\partial t}u(x,t) + \frac{\partial}{\partial x}f(u(x,t)) = 0 \tag{1}$$

where $u(x,t)$ is a conserved quantity, or state variable, while $f(u)$ is called flux function.

An important class of methods for solving hyperbolic conservation laws are the Godunov-type methods, that use, in some way, an exact or approximate solution of the Riemann problem and do not produce oscillations around strong discontinuities such as shocks or contact discontinuities. But these methods are only first order and so the solutions are smoothed around discontinuities. Therefore other methods have been developed, which are at least second-order accurate on smooth solutions and attempt to control the generation of overshoots or undershoots in the vicinity of shocks. These methods are called *high resolution methods* and can be viewed as an extension of Godunov's approach ([1, 3, 4, 6, 8, 9]).

This paper is organized as follows. In the next Section one-dimensional hyperbolic conservation laws are introduced and studied. Furthermore, classical and weak solutions are defined and the Riemann problem is introduced and solved. The Riemann problem forms the underlying physical model for the Godunov-type methods. In Section 3 Godunov's method, proposed by Godunov in 1959, and van Leer's method, an example of high resolution method, are discussed. In the last Section, we test both methods with linear and non linear problems, to compare their different behavior in presence of shock and discontinuous solutions. As non linear problem, we consider Burgers' equation because it is an important test for numerical methods dealing with nonlinear PDEs.

2 Hyperbolic Conservation Laws

2.1 Integral and Differential Form

Equation (1) derives from physical principles. As an example, we consider the equation for conservation of mass in a one-dimensional gas dynamics problem, i.e., flow in a tube where properties of the gas such density and velocity are assumed to be constant across each section of the tube.

Let x represent the distance along the tube and let $\rho(x,t)$ be the density of the gas at point x and time t. This density is defined in such a way the total mass of gas in any given section from x_1 to x_2 is given by the integral of the density. By assuming that the walls of the tube are impermeable and the mass is neither created nor destroyed, the mass in this one section can change only because of gas flowing across the endpoints x_1 or x_2.

Let $v(x,t)$ be the velocity of the gas at the point x and time t. Then the rate of flow, or flux of gas past in this point, is given by the product $\rho(x,t)v(x,t)$.

Then the rate of change of mass in $[x_1, x_2]$ is given by the difference in fluxes at x_1 and x_2:

$$\frac{d}{dt}\int_{x_1}^{x_2} \rho(x,t)dx = \rho(x_1,t)v(x_1,t) - \rho(x_2,t)v(x_2,t)$$

So, we obtain an integral form of the conservation law. By integrating this in time from t_1 to t_2 ($t_2 > t_1$) we obtain:

$$\int_{x_1}^{x_2} \rho(x,t_2)dx =$$

$$= \int_{x_1}^{x_2} \rho(x,t_1)dx + \int_{t_1}^{t_2} \rho(x_1,t)v(x_1,t)dt - \int_{t_1}^{t_2} \rho(x_2,t)v(x_2,t)dt$$

To obtain the differential form of the conservation law, we assume that the functions ρ and v are differentiable functions.

Then, the following equalities hold:

$$\int_{t_1}^{t_2} \frac{\partial}{\partial t}\rho(x,t)dt = \rho(x,t_2) - \rho(x,t_1)$$

and

$$\int_{x_1}^{x_2} \frac{\partial}{\partial x}(\rho(x,t)v(x,t))dx = \rho(x_2,t)v(x_2,t) - \rho(x_1,t)v(x_1,t).$$

By substituting these expressions in the previous equation, we obtain:

$$\int_{t_1}^{t_2}\int_{x_1}^{x_2} \{\frac{\partial}{\partial t}\rho(x,t) + \frac{\partial}{\partial x}(\rho(x,t)v(x,t))\}dxdt = 0.$$

Since this must hold for any section $[x_1, x_2]$ and over any time interval $[t_1, t_2]$, we conclude that the integrand of this equation must be identically zero, i.e.,

$$\rho_t + (\rho v)_x = 0$$

This is the differential form of the conservation law for the conservation of the mass and can be solved in isolation only if the velocity $v(x,t)$ is known a priori or is known as a function of $\rho(x,t)$ (in this case we have a scalar conservation law for ρ), otherwise we can solve this equation in conjunction with other equations, typically with equations for the conservation of momentum and energy, and so we have a system of conservation laws.

As example of scalar conservation law, we consider the flow of cars on a highway. So, ρ denote the density of cars and v the velocity. We can assume that v is a given function of ρ because on a highway we would optimally like to drive at some speed v_{max} (the speed limit), but in heavy traffic we slow down, with velocity decreasing as density increasing. The simplest model is the linear relation

$$v(\rho) = v_{max}(1 - \rho/\rho_{max})$$

where ρ_{max} is the value at which cars are bumper to bumper. Therefore, setting $f(\rho) = \rho v_{max}(1 - \rho/\rho_{max})$, we obtain the scalar conservation law $\rho_t + (f(\rho))_x = 0$ (see [8]).

2.2 Classical and Weak Solutions

The equation (1) must be augmented by some initial conditions and also possibly boundary conditions on a bounded spatial domain. The simplest problem is the initial value problem, or *Cauchy problem*, defined for $-\infty < x < \infty$ and $t \geq 0$. We must specify initial conditions only:

$$u(x,0) = u_0(x) \qquad -\infty < x < \infty \tag{2}$$

It is very easy to see that classical solutions of (1)-(2) are constant along the *characteristics*, which are curves $(x(t),t)$ defined by

$$\begin{cases} \dfrac{dx}{dt} = f'(u(x(t),t)) \quad t \geq 0 \\ x(0) = x_0 \end{cases} \tag{3}$$

To see this, differentiate $u(x,t)$ along one of these curves: in this way, we find the rate of change of u along the characteristics and we find that

$$\begin{aligned} \frac{d}{dt}u(x(t),t) = \; & \frac{\partial}{\partial t}u(x(t),t) + \frac{\partial}{\partial x}u(x(t),t)x'(t) \\ & = u_t + f'(u)u_x \\ & = u_t + (f(u))_x \\ & = 0, \end{aligned}$$

confirming that u is constant along these characteristics. Moreover, this shows that the characteristics travel at constant velocity which is equal to $f'(u_0(x_0))$.

Simple arguments show that if $u_0(x)$ is increasing (decreasing) and $f(u)$ is convex (concave), the classical solution of (1)-(2) is well defined for all $t > 0$. However, in the general case, classical solutions fail to exist for all $t > 0$ even if u_0 is very smooth (see [8, 9]). This happens when $\inf_x u_0'(x)f''(u_0(x)) < 0$: then classical solutions exist only for t in $[0, T^*]$ where

$$T^* = -\frac{1}{\inf_x u_0'(x)f''(u_0(x))}.$$

At the time $t = T^*$ the characteristics first cross, the function $u(x,t)$ has an infinite slope – the wave is said to *break* by analogy with waves on a beach – and a shock forms.

We state this result in the following theorem.

Theorem 2.1 *If we solve (1)-(2) with smooth initial data $u_0(x)$ for which $u_0'(x)f''(u_0(x)$ is somewhere negative, then the wave will break at time*

$$T^* = -\frac{1}{\inf_x u_0'(x)f''(u_0(x))}.$$

Proof. Since along characteristics $u(x(t),t)$ is equal to $u_0(x_0)$, we can write $x(t) = x_0 + tf'(u_0(x_0))$. We can calculate the blow up time (i.e., the first time when two differ-

ent characteristics arrive at same point (x,t)). In this case there are two points, x_0 and $\overline{x}_0$, such that

$$x = x_0 + tf'(u_0(x_0)) = \overline{x}_0 + tf'(u_0(\overline{x}_0)),$$

that is,

$$t = -\frac{\overline{x}_0 - x_0}{f'(u_0(\overline{x}_0)) - f'(u_0(x_0))} = -\frac{1}{u_0'(\xi)f''(u_0(\xi))},$$

where ξ lies between x_0 and $\overline{x}_0$. Obviously, this expression for t makes sense when $\frac{1}{u_0'(\xi)f''(u_0'(\xi))}$ is negative. Thus, the blow up occurs if $u_0'(x)f''(u_0(x)$ is somewhere negative: at $t = T^*$ the solution forms a shock wave. □

To allow discontinuities, which arise in a natural way in this situation, we define a weak solution of conservation law.

Definition 2.2 *A function $u(x,t)$, bounded and measurable, is called a weak solution of the conservation law (1)-(2), if for each $\phi \in \mathcal{C}_0^1(\mathbb{R} \times \mathbb{R}^+)$, the following equality holds:*

$$\int_0^\infty \int_{-\infty}^{+\infty} [\phi_t u + \phi_x f(u)] dx dt = -\int_{-\infty}^{+\infty} \phi(x,0)u(x,0)dx. \tag{4}$$

Here $\mathcal{C}_0^1(\mathbb{R} \times \mathbb{R}^+)$ is the space of functions that are continuously differentiable with compact support, that is, $\phi(x,t)$ is identically zero outside of some bounded set and so the support of the function lies in a compact set.

In this way we rewrite the differential equation in a form where less smoothness is required to define solution. In fact, the basic idea to define a weak solution of conservation law is to take the PDE, multiply by a smooth test function, integrate one or more times over some domain, and then use integration by parts to move derivatives off the function u and onto the smooth test function. The result is an equation involving fewer derivatives on u, and hence requiring less smoothness.

2.3 The Riemann Problem

A Riemann problem is simply the conservation law together with particular initial data consisting of two constant states separated by a single discontinuity,

$$u_0(x) = \begin{cases} u_l & x < 0, \\ u_r & x > 0. \end{cases} \tag{5}$$

As an example, consider Burgers' equation, in which $f(u) = \frac{1}{2}u^2$, so our conservation law becomes:

$$u_t + (\frac{1}{2}u^2)_x = 0. \tag{6}$$

This is also called *inviscid* Burgers' equation, since the equation studied by Burgers also includes a viscous term:

$$u_t + (\frac{1}{2}u^2)_x = \epsilon u_{xx}. \tag{7}$$

Equation (7) is the simplest model that includes the nonlinear and viscous effects of fluid dynamics. The analitic solution is available through a transformation known as the Cole-Hopf transformation, because, around 1950, Hopf, and independently Cole, solved exactly this equation ([2, 7]). Thus Burgers' equation provides an important test for many proposed numerical methods dealing with nonlinear PDEs.

Consider the Riemann problem applied to inviscid Burgers' equation (6), with piecewise constant initial data (5). The form of the solution depends on the relation beetwen u_l and u_r.

First case: $u_l > u_r$.

In this case there is a unique weak solution,

Figure 1: Shock wave: $u_l > u_r$

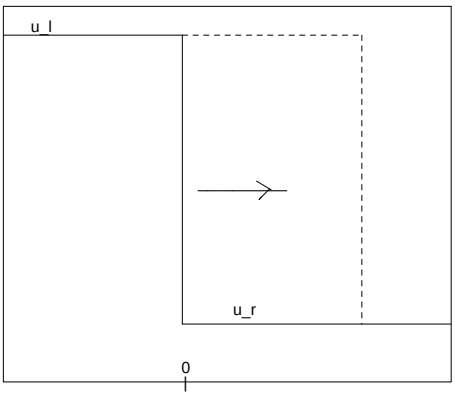

$$u(x,t) = \begin{cases} u_l & x < st \\ u_r & x > st. \end{cases}$$

where

$$s = \frac{(u_l + u_r)}{2}$$

is the shock speed, the speed at which the discontinuity travels.

Second case: $u_l < u_r$.

In this case there are infinitely many weak solutions, since between the points $u_l t < x < u_r t$, there is no information available from characteristics. To determine the correct physical behavior we adopt the vanishing viscosity approach by considering equation (7): equation (7) is a model of (6) valid only for small ϵ and smooth u. If the initial data is smooth and ϵ very

small, then before the wave begins to break the ϵu_{xx} term is negligible compared to other terms and the solutions to both PDEs look nearly identical. As the wave begins to break, the term u_{xx} grows much faster than u_x and at some point the ϵu_{xx} term is comparable to the other terms and begins to play a role. This term keeps the solution smooth for all time, preventing the breakdown of solutions that occurs for the hyperbolic problem. As ϵ goes to zero the solution of the viscous Burgers' equation becomes sharper and sharper and approaches the discontinuous solution of the inviscid Burgers' equation.

Figure 2: Rarefaction wave: $u_l < u_r$

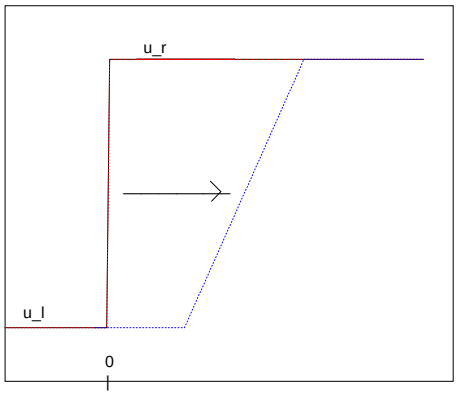

Therefore, to state the weak solution physically correct to this Riemann problem, we consider the solution stable to perturbations and obtained as the vanishing viscosity generalized solution. This is called *rarefaction wave* or *expansion fan* and corresponds to a series of characteristics emanating from the origin with continuous slopes between u_l and u_r:

$$u(x,t) = \begin{cases} u_l & x < u_l t \\ x/t & u_l t \leq x \leq u_r t \\ u_r & x > u_r t \end{cases}$$

So, shock or rarefaction waves are the two possible solutions of the Riemann problem.

More generally, for arbritrary flux function $f(u)$ we have the following relation between the shock speed s and the states u_l and u_r, called *the Rankine-Hugoniot jump condition*:

$$f(u_l) - f(u_r) = s(u_l - u_r). \tag{8}$$

For scalar problems this gives simply

$$s = \frac{f(u_l) - f(u_r)}{u_l - u_r} = \frac{[f]}{[u]}$$

where $[\cdot]$ indicates the jump in some quantity across the discontinuity.

As demonstrated above, there are situations in which the weak solution is not unique and an additional condition is required to pick out the physically relevant vanishing viscosity

solution. Since the condition which defines this solution as the limiting solution of the viscous equations as ϵ goes to zero is not easy to work with, we find simpler conditions. For scalar equations a shock should have characteristics going into the shock, as time advances. A propagating discontinuity with characteristics coming out of it is unstable to perturbations. To this aim the concept of *entropy condition* is introduced. There are general forms of this condition, due to Oleinik, and yet another approach to the entropy condition based on entropy functions (see[1, 8]), but now it is sufficient the following definition:

Definition 2.3 *A discontinuity propagating with speed s given by (8) satisfies the entropy condition if*

$$f'(u_l) > s > f'(u_r).$$

By considering the previous example, when $u_l < u_r$ the entropy condition is violated: in fact, characteristics come out of shock as time advances and the propagating discontinuity is unstable to perturbations. Therefore the solution is not a shock wave but a rarefaction wave.

3 Numerical methods

Let us consider the Cauchy problem for conservation laws (1)-(2). When we attempt to calculate these solutions numerically, new problems arise. A finite-difference discretization of the conservation law (1) is expected to be inappropriate near discontinuities, since it is based on truncated Taylor-series expansions. Indeed, if we compute discontinuous solutions to conservation laws using standard methods, we typically obtain numerical results that are very poor. For example, natural first order accurate numerical methods have a large amount of *numerical viscosity* that smoothes the solution in much the same way physical viscosity would, while a standard second order method eliminates this numerical viscosity but introduces *dispersive effects* that lead to large oscillations in the numerical solution. Therefore we would like to have numerical methods constructed *ad hoc* to solve hyperbolic conservation laws, which are accurate in smooth regions and give good results around shocks. First we consider Godunov's method: it uses the exact solution of the Riemann problem and do not produce oscillations around discontinuities. Unfortunately, it is only first order accurate and so the solutions are very smoothed around discontinuities. A generalization of the Godunov's method is done by the van Leer's method, an example of high resolution method, characterized by second order accuracy on smooth solutions and the absence of spurious oscillations in the computed solution.

Both methods, that we will study in detail, can be written in *conservative* form.

Definition 3.1 *Given a uniform grid with time step Δt and spatial mesh size Δx, a numerical method is said to be conservative if the corresponding scheme can be written as:*

$$v_j^{n+1} = v_j^n - \lambda(g_{j+\frac{1}{2}}^n - g_{j-\frac{1}{2}}^n), \quad j \in \mathbb{Z} \quad n \geq 0 \tag{9}$$

where v_j^n approximates $u(x_j, t_n)$ at the point ($x_j = j\Delta x, t_n = n\Delta t$), $\lambda = \dfrac{\Delta t}{\Delta x}$ and g :

$\mathbb{R}^{2k} \longrightarrow \mathbb{R}$ *is a continuous function, called the* numerical flux *(function), that defines a* $(2k+1)$*-point scheme.*

$$g^n_{j+\frac{1}{2}} = g(v^n_{j-k+1}, \ldots, v^n_{j+k}).$$

The values v^0_j are given by initial conditions.

Essentially, the conservative form ensures that the discretization technique actually represents a discrete approximation to the integral form of the conservation laws, because the time derivative of the integral of v over a given space domain only depends on the boundary fluxes and not on the fluxes within this domain. Now, we can motivate the name of this type of scheme more in detail. This form is very natural if we view v^n_j as an approximation of the average $\overline{u}^n_j$ of $u(\cdot, t_n)$ on the cell $[x_{j-1/2}, x_{j+1/2}]$ (where $x_{j\pm1/2} = x_j \pm \frac{\Delta x}{2}$), defined by

$$\overline{u}^n_j = \frac{1}{\Delta x} \int_{x_{j-1/2}}^{x_{j+1/2}} u(x, t_n) dx.$$

Since the weak solution $u(x,t)$ satisfies the integral form of the conservation law, we have:

$$\begin{aligned} \int_{x_{j-1/2}}^{x_{j+1/2}} u(x, t_{n+1}) dx = & \int_{x_{j-1/2}}^{x_{j+1/2}} u(x, t_n) dx \\ & -[\int_{t_n}^{t_{n+1}} f(u(x_{j+1/2}, t)) dt - \int_{t_n}^{t_{n+1}} f(u(x_{j-1/2}, t)) dt]. \end{aligned}$$

Dividing by Δx and using the averages $\overline{u}^n_j$ this gives

$$\overline{u}^{n+1}_j = \overline{u}^n_j - \frac{1}{\Delta x}[\int_{t_n}^{t_{n+1}} f(u(x_{j+1/2}, t)) dt - \int_{t_n}^{t_{n+1}} f(u(x_{j-1/2}, t)) dt].$$

Comparing this to (9), we see that the numerical flux function can be considered as an average flux through $x_{j+1/2}$ over the time interval $[t_n, t_{n+1}]$,

$$\overline{g}^n_{j+1/2} = \frac{1}{\Delta t} \int_{t_n}^{t_{n+1}} f(u(x_{j+1/2}, t)) dt.$$

An other important property of our numerical methods is the *consistency* with the original conservation law, that is the numerical flux function g reduces to the true flux f for the case of constant flow:

$$g(u, u, \ldots, u) = f(u) \quad \forall u \in \mathbb{R}\,.$$

For consistency it suffices to have g a Lipcschitz continuous function of each variable, i.e. there is a constant $\mathcal{K}$ such that

$$|g(u_{j-k+1}, \ldots, u_{j+k}) - f(u)| \leq \mathcal{K} \max_{-k+1 \leq i \leq k} |u_{j+i} - u|,$$

for all u_{j+i} sufficiently close to u.

The main advantage of conservative and consistent schemes is that, when they converge, they converge to solutions whose shocks or discontinuity satisfy automatically the jump conditions, that is, the discontinuities always travel at the correct velocity. This important result, which is not true for non conservative or non consistent schemes, is due to Lax and Wendroff (the proof is given in [8]).

Theorem 3.2 (Lax-Wendroff) *Assume that the scheme (9) is consistent with the conservation law (1)-(2) and that it generates a sequence that converge to a function u^* as the gridsizes Δx, Δt go to zero. Then, u^* is a weak solution of the conservation law.*

3.1 Godunov's method

Godunov's method is an example of conservative scheme. In this method, the solution is considered as piecewise constant over each mesh cell at a fixed time and the evolution of the solution to the next time step results from the wave interactions originating at the boundaries between adjacent cells. The cell interfaces separate two different states at the left and at the right side, and the resulting local interaction can be exactly resolved since the initial conditions at time $t = n\Delta t$ correspond to the Riemann problem. In order to define completely the interaction between adjacent cells, the time interval over wich the waves are allowed to propagate should be limited by the condition that adjacent Riemann problems do not interfere. This leads to a form of CFL condition.

Godunov's method can be described as follows ([1, 3, 8]):

1. Given data v_j^n at time t_n, construct a piecewise constant function $\hat{v}_j^n(x, t_n)$ defined by

$$\hat{v}_j^n(x, t_n) = v_j^n \qquad x_{j-1/2} \leq x \leq x_{j+1/2}. \tag{10}$$

Figure 3: First stage of Godunov scheme at time t_n

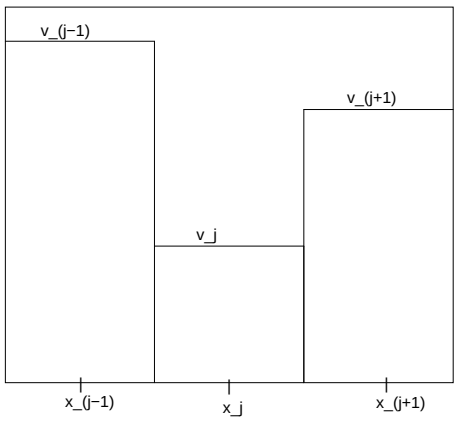

2. Solve the local Riemann problem at the cell interfaces, that is, on each subinterval $[x_j, x_{j+1}]$ and for $t \geq t_n$, solve

$$\begin{cases} \dfrac{\partial}{\partial t}\hat{v}_j^n + \dfrac{\partial}{\partial x} f(\hat{v}_j^n) = 0 \\ \hat{v}_j^n(x, t_n) = \begin{cases} v_j^n, & x_j < x < x_{j+1/2} \\ v_{j+1}^n, & x_{j+1/2} < x < x_{j+1} \end{cases} \end{cases} \tag{11}$$

3. Define the approximation v_j^{n+1} at time t_{n+1} by averaging the Riemann problem solution $\hat{v}_j^n$ at the time t_{n+1}, so

$$v_j^{n+1} = \frac{1}{\Delta x} \int_{x_{j-1/2}}^{x_{j+1/2}} \hat{v}_j^n(x, t_{n+1}) dx. \tag{12}$$

These values are then used to define new piecewise constant data $\hat{v}_j^{n+1}(x, t_{n+1})$ and the process repeats.

The first and third stages are of numerical nature and can be considerd as a *projection steps*, independent of the second, physical, stage, the *evolution step*.

Figure 4: Linear convection: translation of discontinuity

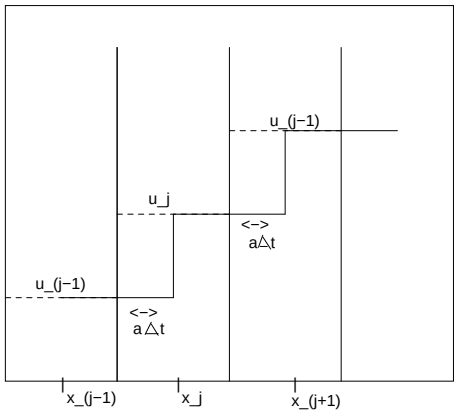

The basic steps of the Godunov approach can best be made clear when applied to the simple linear advection equation $u_t + au_x = 0$, with $a > 0$. The first step is independent of the equation to be solved. The second, physical, step is obtained from the exact solution of the equation at the interface. For the linear advection equation, the discontinuity at the interface is translated over the distance $a\Delta t$ without modification, resulting in the situation shown in Figure 4. The new approximation at time level $n + 1$ results from the averaging of this new state. Since the exact linear solution is

$$\hat{v}^n(x, t) = u^n[x - a(t - n\Delta t)],$$

the new average value in cell i is obtained as

$$\begin{aligned} v_i^{n+1} &= \frac{1}{\Delta x}\int_{x_{i-1/2}}^{x_{i+1/2}} u^n(x - a\Delta t)dx \\ &= \frac{1}{\Delta x}[a\Delta t v_{i-1}^n + (\Delta x - a\Delta t)v_i^n] \\ &= v_i^n - a\frac{\Delta t}{\Delta x}(v_i^n - v_{i-1}^n) \end{aligned}$$

In practice the Godunov's scheme is equal to the first-order upwind scheme when we solve the linear advection equation.

More in general, provided we assume the CFL condition

$$\lambda \max_u |f'(u)| \leq \frac{1}{2},$$

so that the waves issued form the points $x_{j-1/2}$ and $x_{j+1/2}$ do not interact, the solution is obtained by solving a juxtaposition of local Riemann problems and

$$\hat{v}_j^n(x,t) = \hat{v}_R(\frac{x - x_{j+1/2}}{t - t_n}; v_j^n, v_{j+1}^n), \qquad x_j \leq x \leq x_{j+1}, \tag{13}$$

for all $t > t_n$, where $\hat{v}_R$ is the solution of the local Riemann problem.

In order to derive an explicit form of the scheme, let us integrate the equation (11) over the rectangle $(x_{j-1/2}, x_{j+1/2}) \times (t_n, t_{n+1})$. Since the function is piecewise smooth, we obtain:

$$\int_{x_{j-1/2}}^{x_{j+1/2}} (\hat{v}_j^n(x, t_{n+1}) - \hat{v}_j^n(x, t_n))dx + \int_{t_n}^{t_{n+1}} (f(\hat{v}_j^n(x_{j+1/2}^-, t)) - f(\hat{v}_j^n(x_{j-1/2}^+, t)))dt = 0,$$

where we consider the usual notation $x^+ = \lim_{y \to x^+} x$ and $x^- = \lim_{y \to x^-} x$. Using (10) and (12), we get

$$\Delta x(v_j^{n+1} - v_j^n) + \int_{t_n}^{t_{n+1}} (f(\hat{v}_j^n(x_{j+1/2}^-, t) - f(\hat{v}_j^n(x_{j-1/2}^+, t)))dt = 0$$

At this point we note that the integral we need to compute in the previous equation is trivial because the integrand is independent of t. This follows by using (13) and from the fact that the solution of the Riemann problem at $x_{j+1/2}$ is a similarity solution, constant along each ray $(x - x_{j+1/2})/(t - t_n) = constant$. Therefore we have:

$$v_j^{n+1} = v_j^n - \lambda\{f(\hat{v}_R(0^-; v_j^n, v_{j+1}^n)) - f(\hat{v}_R(0^+; v_{j-1}^n, v_j^n))\}.$$

Since the function $x \longrightarrow f(\hat{v}_R(x; u_l, u_r))$ is continuous at the origin because of the Rankine-Hugoniot conditions, Godunov's method can be written in the conservative form

$$v_j^{n+1} = v_j^n - \lambda\{f(\hat{v}_R(0; v_j^n, v_{j+1}^n)) - f(\hat{v}_R(0; v_{j-1}^n, v_j^n))\}. \tag{14}$$

and its numerical flux is given by

$$g(u,v) = f(\hat{v}_R(0;u,v)). \tag{15}$$

3.2 Van Leer's method

Since the first and thirst steps of Godunov's methods are of a numerical nature, they can be modified without influencing the physical input, for instance by replacing the piecewise constant approximation by a piecewise linear variation inside each cell, leading to the definition of second order space-accurate schemes, as van Leer's method. However, the straightforward replacement of the first-order scheme by appropriate second-order accurate formulae leads to the generation of oscillations around discontinuities. To overcome this limitation and achieve the goal of oscillation-free, second-order schemes able to represent accurately shock and discontinuities, there are introduced non linear components. Non linear discretizations imply that the schemes will be non linear even when applied to linear equations. This concept was introduced initially by van Leer under the form of *limiters*, which control the gradient of the computed solution such as to prevent the appearance of overshoots or undershoots.

Consequently, we study van Leer's method as an example of second-order slope limiter methods. The three main steps of van Leer's scheme are the following ([3, 4, 5]):

1. A *reconstruction step* which consists in constructing a piecewise linear function $\hat{v}$ from given cell averages v_j^n,

$$\hat{v}^n(x) = v_j^n + (x - x_j)\frac{S_j^n}{\Delta x}, \qquad x_{j-1/2} < x < x_{j+1/2}, \tag{16}$$

where S_j^n is a *slope* on the jth cell wich is based on the numerical values at time t_n. Note that taking $S_j^n = 0$ for all j and n recovers Godunov's method.

2. An *evolution step*, which involves either an exact or an approximate Riemann solver. One solves

$$\begin{cases} \dfrac{\partial}{\partial t}w + \dfrac{\partial}{\partial x}f(w) = 0 \quad x \in R, t_n \le t \le t_{n+1} \\ w(x,t_n) = \hat{v}^n(x) \end{cases} \tag{17}$$

which gives $w(\cdot, t_{n+1})$.

3. A *cell-averaging step*, which gives v_j^{n+1}, by projecting the solution $w(x,t_{n+1})$ onto the piecewise constant functions

$$v_j^{n+1} = \frac{1}{\Delta x}\int_{x_{j-1/2}}^{x_{j+1/2}} w(x,t_n)dx. \tag{18}$$

The cell average of $\hat{v}^n(x)$ over $[x_{j-1/2}, x_{j+1/2}]$ is equal to v_j^n for any choice of S_j^n. Since steps 2 and 3 are also conservative, the overall method is conservative for any choice of S_j^n.

Provided we assume some convenient CFL condition so that the waves issued from the points $x_{j-1/2}$ and $x_{j+1/2}$ do not interact, the solution is obtained by juxtaposition of local

Riemann problems. In order to derive a more explicit form of the scheme, we integrate the equation (17) over a cell $(x_{j-1/2}, x_{j+1/2}) \times (t_n, t_{n+1})$,

$$\int_{t_n}^{t_{n+1}} \int_{x_{j-1/2}}^{x_{j+1/2}} (\frac{\partial}{\partial t} w + \frac{\partial}{\partial x} f(w)) dx dt = 0.$$

We obtain

$$\int_{x_{j-1/2}}^{x_{j+1/2}} (w(x, t_{n+1}) - w(x, t_n)) dx + \int_{t_n}^{t_{n+1}} (f(w(x_{j+1/2}, t)) - f(w(x_{j-1/2}, t))) dt = 0$$

since the flux is continuous, and then by (18)

$$\Delta x (v_j^{n+1} - v_j^n) + \int_{t_n}^{t_{n+1}} (f(w(x_{j+1/2}, t)) - f(w(x_{j-1/2}, t))) dt = 0$$

We are left with the evaluation of the numerical flux

$$g_{j+1/2}^n = \frac{1}{\Delta t} \int_{t_n}^{t_{n+1}} f(w(x_{j+1/2}, t)) dt.$$

Using the midpoint rule, we write

$$\frac{1}{\Delta t} \int_{t_n}^{t_{n+1}} f(w(x_{j+1/2}, t)) dt = f(w(x_{j+1/2}, t_n + \frac{\Delta t}{2})) + \mathcal{O}(\Delta t^2).$$

A way for approximating $f(w(x_{j+1/2}, t_n + \frac{\Delta t}{2}))$ is given by a predictor-corrector scheme. Following an idea of Hancock, we define the updated values $v_{j+1/2,\pm}^{n+1/2}$ at time $t_n + \frac{\Delta t}{2}$ by

$$\begin{cases} v_{j+1/2,-}^{n+1/2} = v_{j+1/2,-}^n - \dfrac{\Delta t}{2\Delta x} (f(v_{j+1/2,-}^n) - f(v_{j-1/2,+}^n)), \\ \\ v_{j+1/2,+}^{n+1/2} = v_{j+1/2,+}^n - \dfrac{\Delta t}{2\Delta x} (f(v_{j+3/2,-}^n) - f(v_{j+1/2,+}^n)), \end{cases}$$

where

$$\begin{cases} v_{j+1/2,-}^n = \hat{v}(x_{j+1/2}^-) = v_j^n + \dfrac{S_j^n}{2}, \\ v_{j+1/2,+}^n = \hat{v}(x_{j+1/2}^+) = v_{j+1}^n - \dfrac{S_{j+1}^n}{2}, \end{cases}$$

Then, we solve the Riemann problem at the point $x_{j+1/2}$ with piecewise constant initial data $v_{j+1/2,\pm}^{n+1/2}$

$$\begin{cases} \dfrac{\partial}{\partial t} \hat{w} + \dfrac{\partial}{\partial x} f(\hat{w}) = 0 \\ \hat{w}(x, 0) = \begin{cases} v_{j+1/2,-}^{n+1/2} & x < x_{j+1/2} \\ v_{j+1/2,+}^{n+1/2}, & x > x_{j+1/2} \end{cases} \end{cases}$$

whose solution is noted as $v_R(\frac{x - x_{j+1/2}}{t}; v^{n+1/2}_{j+1/2,-}, v^{n+1/2}_{j+1/2,+})$.

We replace

$$w(x_{j+1/2}, t)$$

by

$$v_R(0; v^{n+1/2}_{j+1/2,-}, v^{n+1/2}_{j+1/2,+}),$$

and thus we take

$$g^n_{j+1/2} = f(v_R(0; v^{n+1/2}_{j+1/2,-}, v^{n+1/2}_{j+1/2,+})).$$

It remains to solve the problem of definition of S^n_j. In fact the main difficulty in obtaining a slope limiter method is the choice of the slopes S^n_j. For example, it can be shown that for the linear advection equation with $f(u) = au$ and $a > 0$, if $S^n_j = v^n_{j+1} - v^n_j$ and the advection equation is solved exactly in step 2, then the method reduces to the Lax-Wendroff method (see [8]). This illustrates that it is possible to obtain second order accuracy by this approach. The oscillations which arise with Lax-Wendroff method can be interpreted geometrically as being caused by a poor choice of slopes. In fact oscillations are created when the slope in a cell becomes larger than the difference of adjacent mean values. Hence, in order to define a scheme without overshoots around discontinuities one should avoid excessive large gradients. Therefore we have to make a controll at each time step and within each cell, in such a way as to keep the gradients within the proper bounds. So, we prevent the generation of oscillations by acting on their production mechanism and we introduce nonlinear correction factors, the limiters.

In this way, the method is TVD (Lax-Wendroff scheme is not TVD).

Briefly, we report the definition of a *total variation diminishing* (TVD) numerical method:

Definition 3.3 *A numerical method to solve hyperbolic conservation laws is called total variation diminishing if*

$$\sum_{j=-\infty}^{+\infty} |v^{n+1}_{j+1} - v^{n+1}_j| \leq \sum_{j=-\infty}^{+\infty} |v^n_{j+1} - v^n_j|$$

The advantage of a TVD scheme stems from the fact that, whenever stability is assured, it is free of numerical oscillations.

To obtain a slope limiter we can set

$$S^n_j = (v^n_{j+1} - v^n_j)\Phi^n_j$$

where $\Phi_j = \Phi(\theta^n_j)$ and θ^n_j represents the ratio of consecutive gradients,

$$\theta_j^n = \frac{v_j^n - v_{j-1}^n}{v_{j+1}^n - v_j^n},$$

while Φ is a limiter function, defined to obtain a TVD method. We set:

$$\Phi(\theta) = 0 \qquad \text{for } \theta \leq 0.$$

With these assumptions, we have the sufficient condition to obtain a TVD scheme:

$$0 \leq \Phi(\theta) \leq 2\theta.$$

To obtain second order accuracy, additional conditions are to be imposed , for example, the function Φ must also pass smoothly through the point $\Phi(1) = 1$. Various limiter functions have been defined in the literature. Actually, we consider three limiter functions:

- van Leer's limiter:

$$\Phi(\theta) = \frac{|\theta| + \theta}{1 + |\theta|}$$

- *minmod* limiter that represents the lowest boundary of the second-order TVD region:

$$\Phi(\theta) = \begin{cases} \min(\theta, 1) & \text{if } \theta > 0 \\ 0 & \text{if } \theta \leq 0 \end{cases}$$

  It is a particular case of the minmod function, defined as the function that selects the number with the smallest modulus from a series of numbers when they all have the same sign, and zero otherwise. For two arguments:

$$\text{minmod}(x, y) = \begin{cases} x & \text{if } |x| < |y| \quad \text{and } xy > 0 \\ y & \text{if } |x| > |y| \quad \text{and } xy > 0 \\ 0 & \text{if } xy < 0 \end{cases}$$

- the *superbee* limiter, that represents the upper limit of the second-order TVD region and has been introduced by Roe:

$$\Phi(\theta) = \max[0, \min(2\theta, 1), \min(\theta, 2)].$$

4 Numerical results

Now, we investigate how the previously analyzed methods (Godunov and van Leer's schemes) behave in practice when applied to different model problems. We have chosen the linear advection equation, which serves as a simple model for contact discontinuities in fluid dynamics, and Burgers' equation to study how the methods treat shocks. To apply any of the methods in

a finite domain, we are immediately faced with the problem of how to discretize the equations at the boundary points.

First of all, we impose periodic boundary conditions,

$$u(x_{min}, t) = u(x_{max}, t),$$

so that we use periodicity conditions to provide the extra needed values for implement Godunov and van Leer's schemes. In this way we overcome the difficulty that arise near the boundaries ([3, 4, 5]).

Example 1

We begin by studying the simple hyperbolic equation

$$\begin{array}{ll} u_t + u_x = 0 & x \in [-1, 1] \quad t \geq 0 \\ u(x, 0) = u_0(x) = sin(2\pi x) & x \in [-1, 1] \end{array}$$

Its exact solution is the wave $u(x, t) = sin(2\pi(x - t))$, constant along the characteristics $x - t = constant$, and with speed of propagation equal to $dx/dt = 1$.

In this case the CFL number is $\lambda = \Delta t/\Delta x$, because $max|f'(u)| = 1$.

We calculate the solution at time $t = 2$ with a CFL number equal to $\lambda = 0.5$, with $\Delta t = 2/200$ and $\Delta x = 2/100$. Figure 5 shows numerical solutions to this problem computed with Godunov and van Leer's method: the results are plotted at time $t = 2$ along with exact solution. It is evident that Godunov's method gives very smeared solutions because it is a first order method, while van Leer's method well approximates exact solution. Also, we can compare the specific effects of the limiters on smooth solutions: the minmod limiter reduces locally the accuracy of the solution around the extrema and the behavior is close to a first order method, while superbee limiter flattens the maxima. The overcompressive property of superbee limiter is not too adequate for smooth profiles. Instead, the van Leer limiter has properties between minmod and superbee limiters' properties.

Example 2

To simulate contact discontinuities we again solve the linear advection equation $u_t + u_x = 0$, with initial condition $u_0(x)$ periodic of period 2 defined on the interval $[-1, 1]$ as

$$u_0(x) = \begin{cases} 1 & -1 \leq x \leq -0.75 \\ 0 & -0.75 < x < -0.25 \\ 1 & -0.25 \leq x \leq 0.25 \\ 0 & 0.25 < x < 0.75 \\ 1 & 0.75 \leq x \leq 1 \end{cases}$$

We solve this problem at time $t = 2$ with $\lambda = 0.5$, by setting $\Delta t = 2/200$ and $\Delta x = 2/100$. The expected behavior of numerical methods considered is plotted in figure 6.

Godunov's scheme shows excessive diffusion, while van Leer, minmod and superbee limiters generate monotone profiles. The minmod limiter, however, is still too diffusive.

Example 3

Figure 5: Example (1): numerical $(-\cdot-)$ and exact $(-)$ solution with $\lambda = 0.5$ and $\Delta x = 2/100$

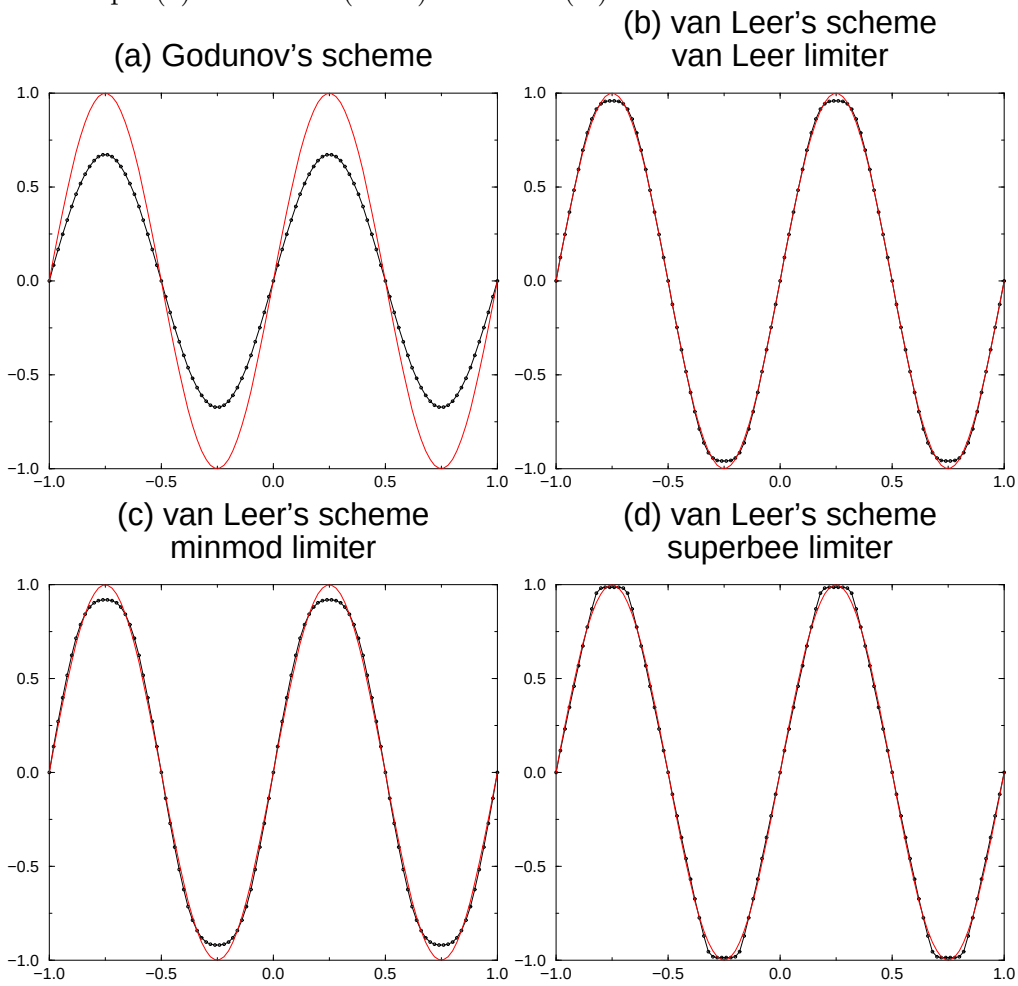

As nonlinear test problem with periodic initial and boundary conditions, we consider inviscid Burgers' equation (6) on the interval $[0, 2\pi]$ and $t \geq 0$, with periodic boundary conditions $u(0,t) = u(2\pi,t)$ and initial condition $u_0(x) = 5/2 + \sin x$. As t increases from the origin, $u_0(x)$ is transported with unit speed to the right and simultaneously evolves into a function with an increasingly sharper profile which, after a while, is discontinuous: a shock appears. Figure 7 displays the initial condition. The evolution of the solution of this Burgers' equation at times $t = 0.2,\ 0.4,\ 0.8,\ 1,\ 1.2,\ 1.4,\ 1.6,\ 2$ is plotted in Figure 8 by applying Godunov's method, while in Figure 9 solution obtained by applying van Leer's method with van Leer limiter is displayed. We have chosen van Leer limiter, because its behavior is between the minmod and superbee limiters' behavior. For both method we have chosen $\Delta t = 0.002$ and $\Delta x = 2\pi/100$.

We see how a smooth solution degenerates into a discontinuous one. But Godunov's method tends to smooth the profile while van Leer's method is more efficient to control the shock.

If we have more general initial conditions, we have to study how many conditions of physical origin are to be imposed at a given boundary and how many numerical conditions are to be defined at the boundaries. A particular attention is needed to the study of the

Figure 6: Example (2): numerical ($-\cdot-$) and exact ($-$) solution with $\lambda = 0.5$ and $\Delta x = 2/100$

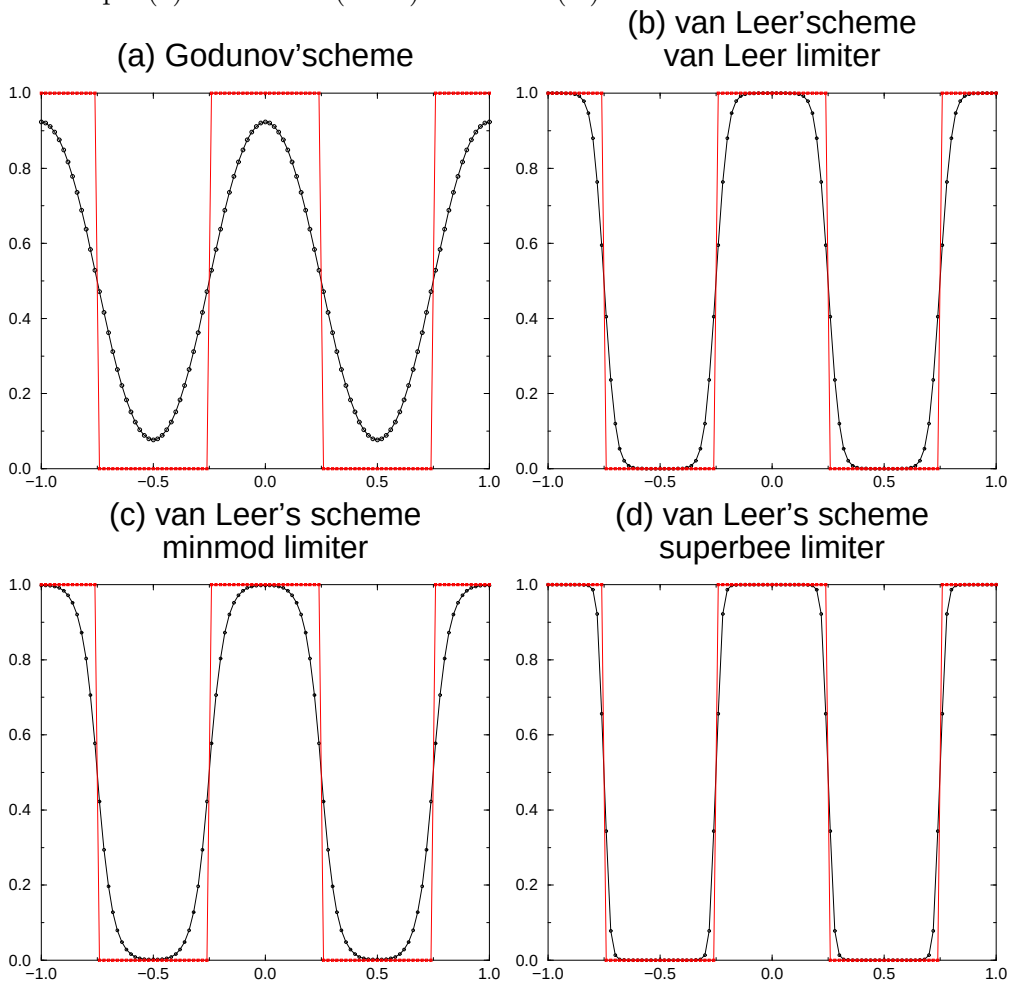

boundary treatment on the stability and accuracy of the basic scheme, since stable schemes can be strongly affected by unadapted boundary treatments, leading to possible instability of the complete scheme or to the reduction of unconditional to conditional stability. Whit regard to accuracy, an important theorem by Gustafsson (see [5]) proves that, for linear equations, the boundary scheme can be one order lower than the basic scheme without reducing the global order of accuracy of the complete scheme.

So we consider the scalar conservation law

$$\begin{aligned} &u_t + (f(u))_x = 0, \qquad x \in [x_{min}, x_{max}],\ t > 0 \\ &u(x,0) = u_0(x), \end{aligned}$$

and we prescribe $u(x_{min}, t) = g(t)$ if the characteristic is ingoing. that is, if $f' > 0$, otherwise we impose $u(x_{max}, t) = g(t)$. For example, if we consider the linear advection equation $u_t + au_x = 0$, if $a > 0$, the characteristics are leaving from the boundary $x = x_{min}$, thus coming into the domain. Therefore, we prescribe the solution at the boundary $x = x_{min}$,

Figure 7: Example (3). Initial condition

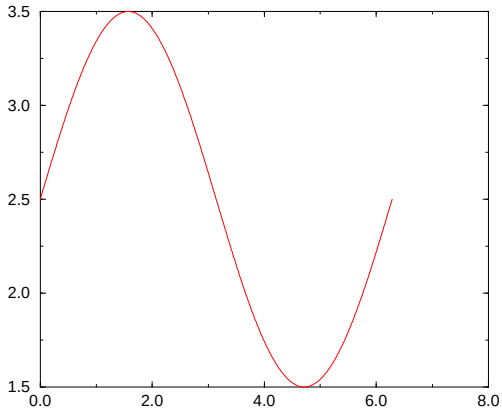

Figure 8: Example (3). Evolution in time by Godunov's method

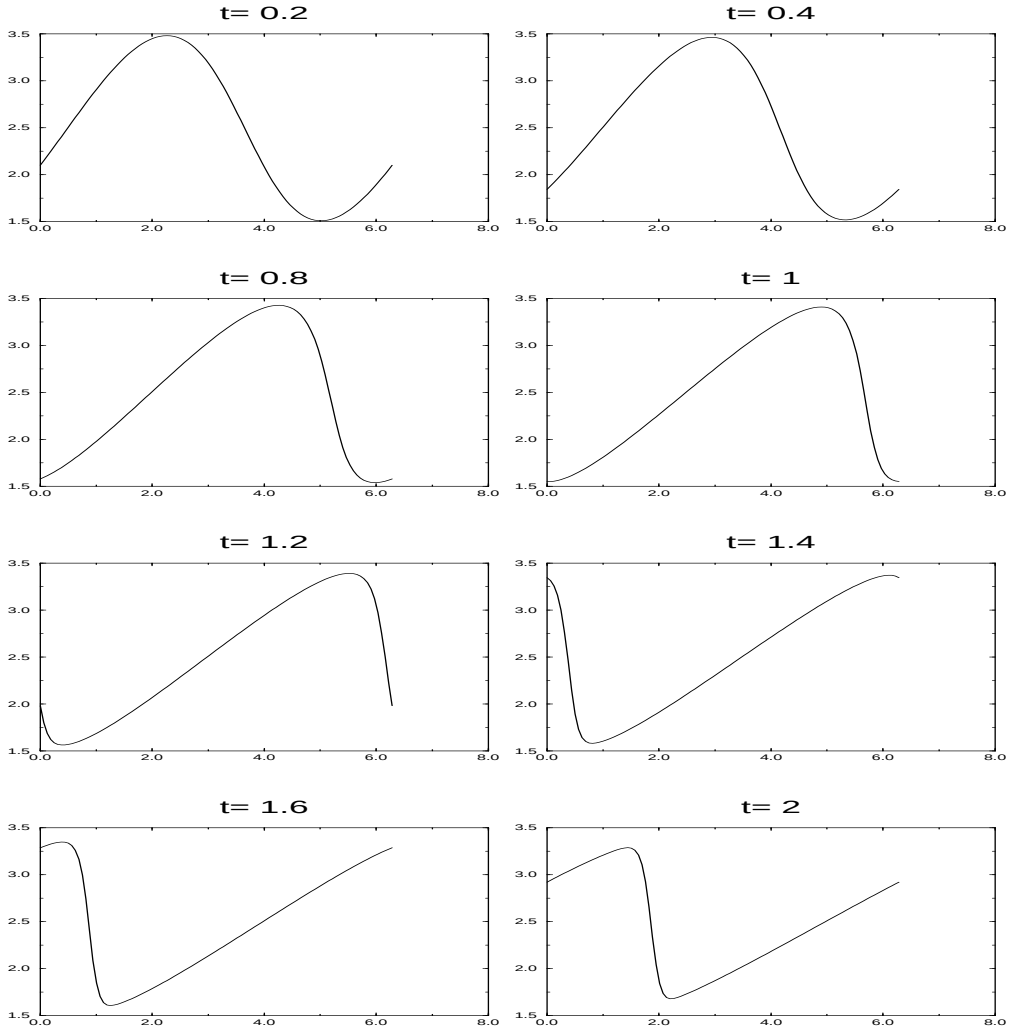

Figure 9: Example (3). Evolution in time by van Leer's method with van Leer limiter

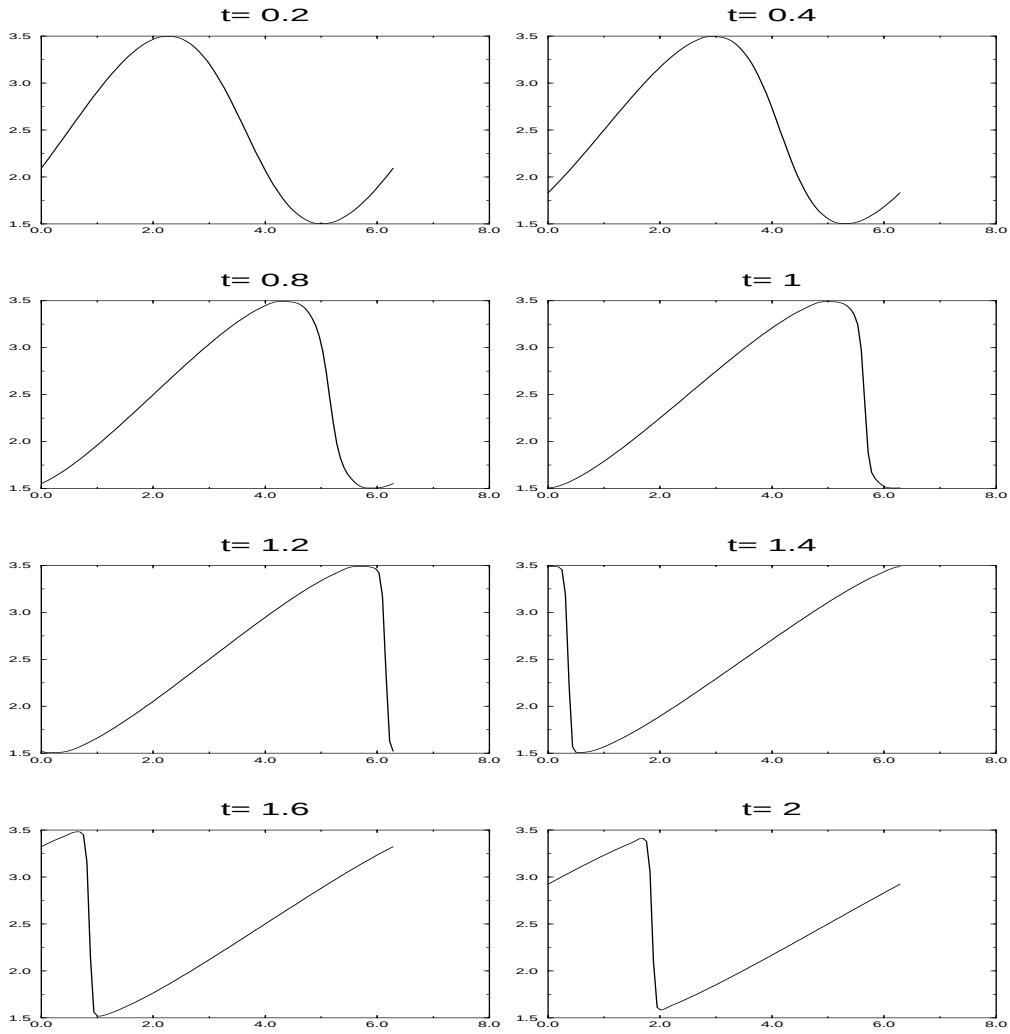

$$u(x_{min}, t) = g(t),\ t > 0.$$

Instead, if $a < 0$ we have

$$u(x_{max}, t) = g(t),\ t > 0.$$

Therefore, when we consider the numerical scheme, at most one of the boundary values is known by analytical boundary conditions. There are some problems with numerical approximations of values near the boundary. Let us divide the space interval $[x_{min}, x_{max}]$ into $N-1$ cells of length Δx, ranging from $j = 1$ at $x = x_{min}$ to $j = N$ at $x = x_{max}$, and consider a 3-point linear conservative scheme as Godunov's scheme for approximating the simple advection equation with $a > 0$.

The formula is:

$$v_j^{n+1} = v_j^n - \lambda(g_{j+\frac{1}{2}}^n - g_{j-\frac{1}{2}}^n),$$

with $g_{j+\frac{1}{2}}^n = g(v_j^n, v_{j+1}^n)$, and j varying from 2 to $N-1$, since v_1^n is given by boundary condition, $v_1^n = g(t_n)$, and the formula cannot be write for $j = N$ because it requires values outside of the computational domain. In the same way, if we use a 5-point scheme, as the van Leer's scheme, we still set $v_1^n = g(t_n)$, and to compute v_2^n and v_{N-1}^n, we need the auxiliary values v_0^n and v_N^n, v_{N+1}^n respectively. Various methods can be applied in order to implement numerical boundary conditions. We consider schemes based on extrapolations of the internal variables toward the boundary. In particular, we consider the following formulae (we write the conditions for an outlet boundary $j = N$. The transposition to inlet conditions is straightforward, replacing $j = N$ by $j = 1$, $j = N - 1$ by $j = 2$ and so on):

- space extrapolation
  - zero-order extrapolation: $v_N^{n+1} = v_{N-1}^{n+1}$
  - first-order extrapolation: $v_N^{n+1} = 2v_{N-1}^{n+1} - v_{N-2}^{n+1}$
- space-time extrapolation
  - zero-order: $v_N^{n+1} = v_{N-1}^n$
  - first order in space/zero order in time: $v_N^{n+1} = 2v_{N-1}^n - v_{N-2}^n$
  - first order in space and time: $v_N^{n+1} = 2v_{N-1}^n - v_{N-2}^{n-1}$
- time extrapolation
  - zero order: $v_N^{n+1} = v_N^n$
  - first order: $v_N^{n+1} = 2v_N^n - v_N^{n-1}$

For the 5-point scheme, one can take for v_N^n and v_{N+1}^n the same formula, i.e., the same coefficients in the extrapolation scheme, for example

$$\begin{array}{ll} v_N^{n+1} = 2v_{N-1}^{n+1} - v_{N-2}^{n+1} & \text{and} \\ v_{N+1}^{n+1} = 2v_N^{n+1} - v_{N-1}^{n+1}. & \end{array}$$

In our numerical experiments, we consider the space-time zero order extrapolation in Godunov's method, while, for van Leer's scheme, we use first-order in space and time formula to obtain v_N^{n+1} and v_{N+1}^{n+1} for $n \geq 1$. For $n = 0$ we consider the first order in space and zero order in time formula, because we start by knowing only the initial values for $t = t_0 = 0$. For the auxiliary value v_0^{n+1} we utilize a zero-order space extrapolation. The theory of Gustafsson guarantees stability and accuracy of both methods.

Example 4

As first example of linear advection equation, $u_t + u_x = 0$, with non periodic initial conditions, we examine the following initial condition:

Figure 10: Example (4): numerical $(-\cdot-)$ and exact $(-)$ solution with $\lambda = 0.5$ and $\Delta x = 0.04$ at time $t = 2$

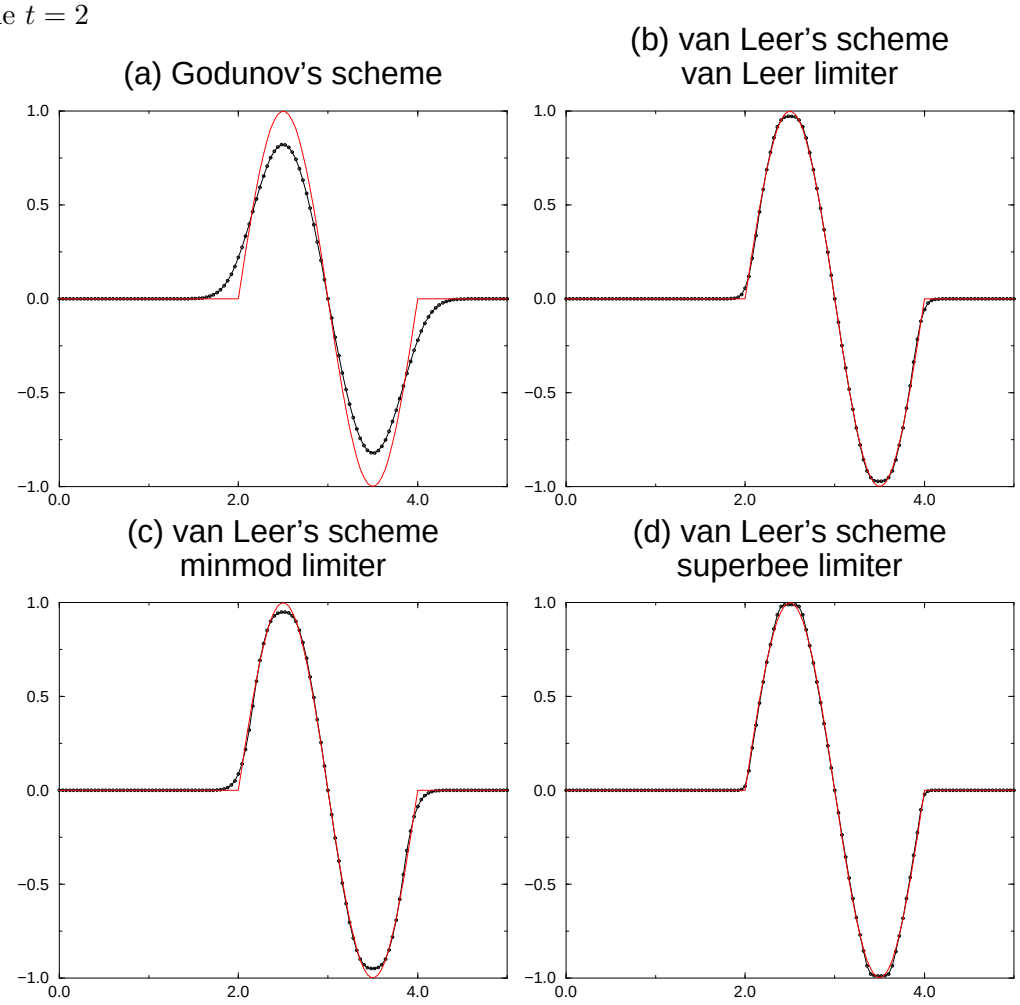

$$u(x,0) = u_0(x) = \begin{cases} \sin(\pi x) & 0 \le x \le 2 \\ 0 & \text{otherwise} \end{cases}$$

This test case allows us to test the diffusion and dispersion properties of the schemes with numerical boundary conditions. As in the case of periodic initial and boundary conditions of example (1), the specific effects of the Godunov's method and of the various limiters applied to van Leer's scheme can be seen from a comparison of Figure 10 where we plot the solution at time $t = 2$: Godunov's scheme presents very smeared solution while the specific effects of the limiters vary from the smoothness of minmod limiter to an overcompressive property of superbee limiter.

Example 5

To study the behavior on shock and contact discontinuities we study the linear advection equation of a square wave. In this case we start by the initial condition:

Figure 11: Example (5) numerical($- \cdot -$) and exact($-$) solution with $\lambda = 0.5$ and $\Delta x = 0.04$ at time $t = 2$

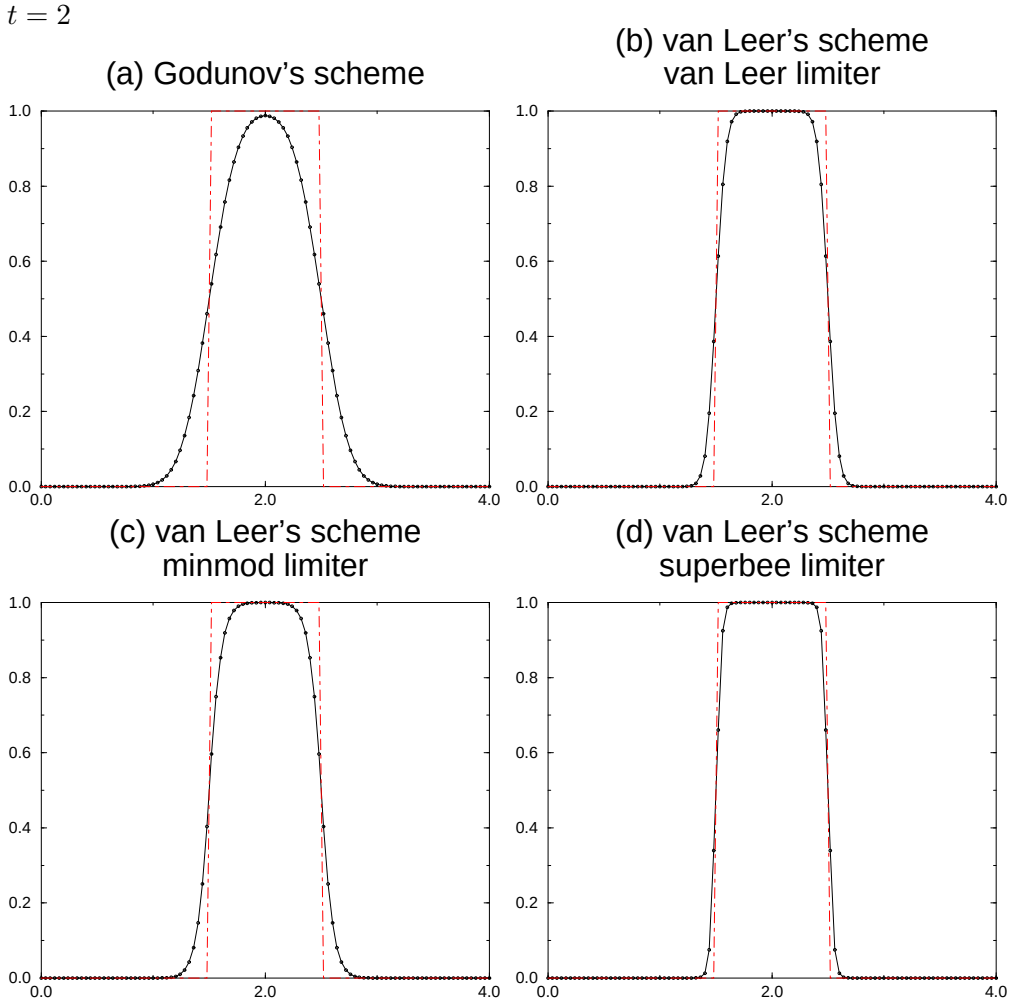

$$u(x,0) = \begin{cases} 1 & -0.5 \le x \le 0.5 \\ 0 & \text{otherwise} \end{cases}$$

In the numerical experiment the space variable x varies in the interval $[-1, 9]$, with $\Delta x = 0.04$ and $\Delta t = 0.02$. Figure 11 compares the linear advection of a square wave after 100 time steps, at time $t = 2$, at a CFL number of 0.5. Godunov's scheme shows excessive diffusion. The minmod limiter is still too diffusive, while the superbee limiter produces excellent results and the van Leer limiter has a behavior between the previous two.

Example 6

As non linear test problem we consider Burgers' equation where shock formation and propagation is provided by the time evolution of a single sinusoidal wave profile:

$$u(x,0) = \begin{cases} 5\sin x & 0 \le x \le \pi \\ 0 & x < 0 \text{ and } x > \pi \end{cases}$$

Figure 12: Example (6). Initial condition

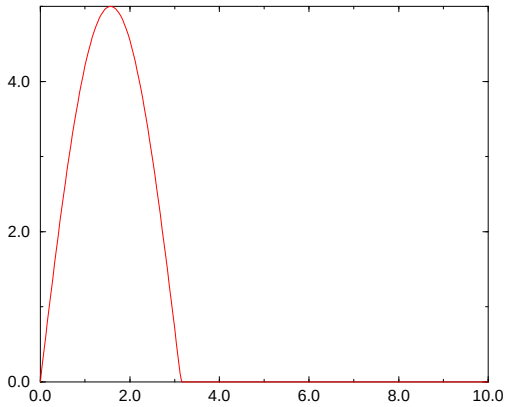

The shock moves at a speed $s = \sqrt{B}t$ and has a jump $[u] = \sqrt{\frac{B}{t}}$, where $B/2$ is the area under the sinusoidal curve, which remains constant, that is

$$B = 2\int_0^{\pi} u(x,0)dx = 20.$$

The expansion part takes on a linear shape asymptotically:

$$u \approx \frac{x}{t}$$

when $0 < x < \sqrt{B}t$. We illustrate the evolution in time in Figure 13, starting by an initial configuration as in Figure 12. The numerical solution for the different methods is obtained with a gridsize $\Delta x = 0.04$ and $\Delta t = 0.004$, at time $t = 5$. In this case $s = 10$ and the jump is equal to 2.

Example 7

Another simple nonlinear test on Burgers' equation is given by considering a Riemann problem, that is, the initial condition is:

$$u(x,0) = \begin{cases} 1 & x < 0 \\ 0 & x > 0 \end{cases}$$

Therefore, we have a shock propagating at speed $s = 1/2$ with unmodified intensity $[u] = 1$. We plot the numerical solution at time $t = 4$, with $\Delta x = 0.04$ and $\Delta t = 0.02$. As expected, Godunov's method presents an oscillatory behavior.

Example 8

As last example we consider the Riemann problem whose solution is a rarefaction wave:

$$u(x,0) = \begin{cases} 0 & x < 0 \\ 1 & x > 0 \end{cases}$$

Figure 13: Example (6): numerical solution with $\lambda = 0.1$ and $\Delta x = 0.04$ at time $t = 5$

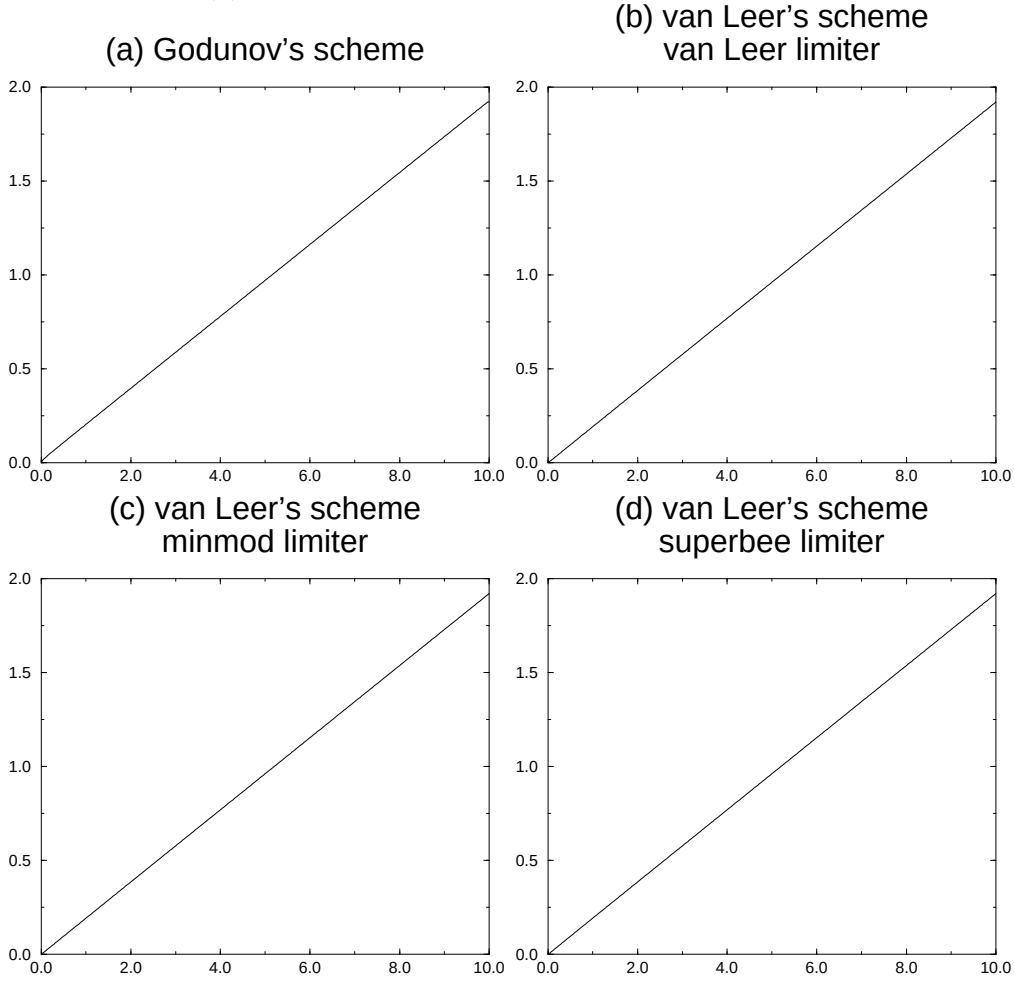

The expected behavior for the methods considered is displayed in Figure 15.

Figure 14: Example (7): numerical $(-\cdot-)$ and exact $(-)$ solution with $\lambda = 0.5$ and $\Delta x = 0.04$

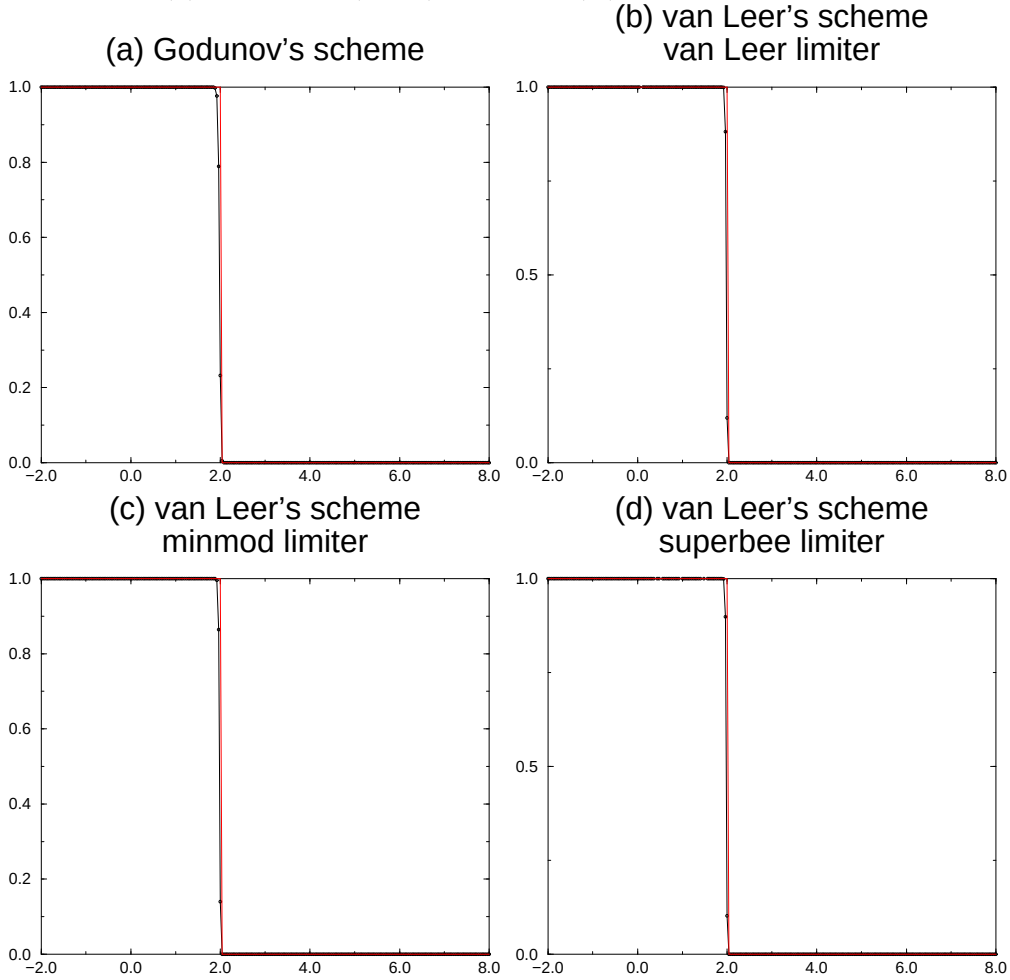

Figure 15: Example (8): numerical ($-\cdot-$) and exact ($-$) solution with $\lambda = 0.5$ and $\Delta x = 0.04$

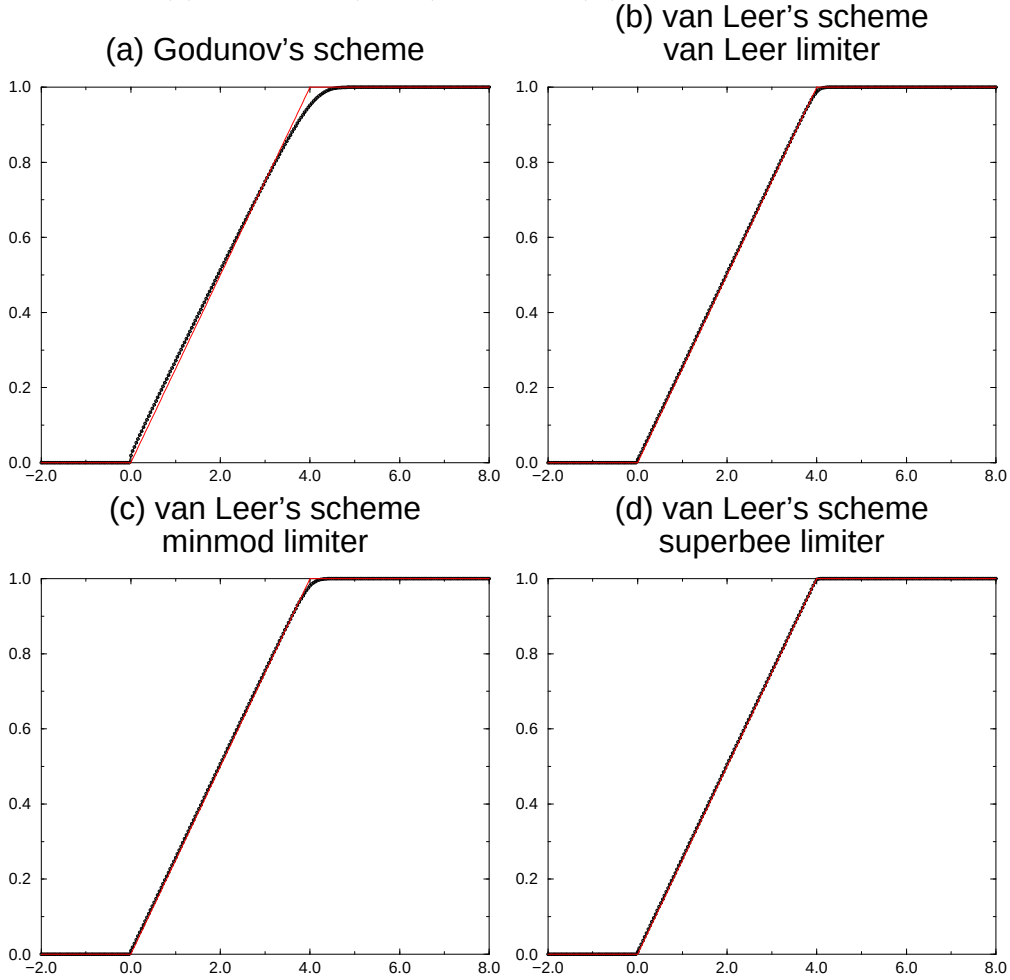

References

[1] A.C. Berkenbosch, E.F. Kaasschieter, J.H.M. ten Thije Boonkkamp, *Finite-Difference Methods for One-Dimensional Hyperbolic Conservation Laws,* Numerical Methods for Partial Differential Equations, **8**, 267-276, (1992).

[2] J.D. Cole, *On a quasilinear parabolic equation occurring in aerodynamics,* Q. Appl. Math. **9**, 225-236 (1951).

[3] E. Godlewski, P.A. Raviart, *Hyperbolic systems of conservation laws,* Mathématiques et Applications, Ellipses, Paris (1991).

[4] E. Godlewski, P.A. Raviart, *Numerical Approximation of Hyperbolic Systems of Conservation Laws,* Springer-Verlag New York, Inc. (1996).

[5] B. Gustaffson, H.O. Kreiss, J. Oliger, *Time Dependent Problems and Difference Methods,* John Wiley & Sons, Inc. (1995).

[6] C. Hirsch, *Numerical Computations of Internal and External Flows,* Vol.2, John Wiley & Sons, Inc. New York(1988).

[7] E. Hopf, *The partial differential equation* $u_t + uu_x = \delta u_{xx}$, Commun. Pure Appl. Math. **3**, 201-230 (1950).

[8] R.J. LeVeque, *Numerical Methods for Conservation Laws,* Lectures in Mathematics, Birkhäuser, Verlag, Basel, (1990).

[9] G.A. Sod, *Numerical Methods in Fluid Dynamics: Initial and Initial Boundary-Value Problems,* Cambridge University Press, (1985).